

$K_1$  is its association constant to dimers.<sup>6</sup> The 30-fold decrease of  $k_{21}/K_2^{1/2}$  compared with  $k_{12}/K_1^{1/2}$  is due to two opposing factors. The more reactive 1,1-diphenylethylene should add more rapidly to the more reactive  $\sim\text{S}^-, \text{Li}^+$  than the less reactive styrene to the less reactive  $\sim\text{D}^-, \text{Li}^+$ , i.e.,  $k_{12}$  is expected to be much larger than  $k_{21}$ . On the other hand, the more bulky  $\sim\text{D}^-, \text{Li}^+$  is expected to be less extensively associated than the less bulky  $\sim\text{S}^-, \text{Li}^+$ , i.e.,  $K_1$  is probably greater than  $K_2$ .

We may also compare  $k_{11}/K_1^{1/2}$  with  $k_{12}/K_1^{1/2}$ ,  $k_{11}$  denoting the bimolecular rate constant of styrene addition to monomeric lithium polystyryl. The value of  $k_{11}/K_1^{1/2}$  is given<sup>2</sup> as  $0.94 \times 10^{-2} \text{ M}^{-1/2} \text{ s}^{-1}$  implying that 1,1-diphenylethylene is twice as reactive as styrene in its addition to monomeric lithium polystyrene.

The importance of mixed dimerization in copolymerization involving Li cations and benzene solvent is shown again in studies of copolymerization of styrene and butadiene. In a paper<sup>7</sup> describing the kinetics of this reaction it was reported that the conversion of lithium butadienyl end group into lithium styryl end group obeys the first-order law. The authors could not explain this result. Apparently even in this system

the association constant of  $\sim\text{S}^-, \text{Li}^+$  and  $\sim\text{B}^-, \text{Li}^+$  (butadienyl group) is again given by the square root of the association constants of the respective homodimerizations. In such a case the treatment outlined in ref 1 and in this paper accounts for the reported kinetic results.

**Acknowledgment.** We wish to thank the National Science Foundation for the generous support of this investigation and the Dow Chemical Company for its unrestricted grant.

## References and Notes

- (1) Z. Laita and M. Szwarc, *Macromolecules*, **2**, 412 (1969).
- (2) D. J. Worsfold and S. Bywater, *Can. J. Chem.*, **38**, 1891 (1960); see also S. Bywater, *Adv. Polym. Chem.*, **4**, 66 (1965).
- (3) A. Yamagishi, M. Szwarc, L. Tung, and G. Y-S Lo, *Macromolecules*, in press.
- (4) G. Spach, H. Monteiro, M. Levy, and M. Szwarc, *Trans. Faraday Soc.*, **58**, 1809 (1962).
- (5) R. Bussion and M. Van Beylen, *Macromolecules*, **10**, 1320 (1977).
- (6) In the original paper of Laita and Szwarc<sup>1</sup> a conversion factor of log into ln was omitted in the calculation. The value of  $k_{12}/K_1$  was checked during the present study and independently was verified by Van Beylen.<sup>5</sup>
- (7) M. Morton and F. R. Ellis, *J. Polym. Sci.*, **61**, 25 (1962).

## Dependence on Molecular Weight of the Chain Expansion Factor of Polystyrene in Dilute Solutions<sup>1</sup>

Hiroyasu Utiyama,\*<sup>2</sup> Shigeo Utsumi, Yoshisuke Tsunashima, and Michio Kurata

*Institute for Chemical Research and Department of Industrial Chemistry, Kyoto University, Kyoto, Japan. Received September 6, 1977*

**ABSTRACT:** Accurate light-scattering and viscosity measurements were made in toluene at 30 °C on five polystyrene samples with narrow distribution in molecular weight. In the range of studied molecular weight, 1.3 million to 15.9 million, it was shown that the double logarithmic plot of  $(\langle S^2 \rangle / M)$  against  $M^{1/2}$  gave a curve concave downward and that the penetration function  $\Psi$  in the expression of  $A_2$  decreased with the expansion factor  $\alpha_s$  with a tendency to level off. The dependence of  $\alpha_s$  on the parameter  $z$  of the excluded-volume effect was deduced from the experimental data in a straightforward way by using the slope  $F$  in the double logarithmic plot of  $(\alpha_s^3 - 1)$  vs.  $M^{1/2}$ . It was concluded that  $F$ , starting from unity at  $\alpha_s = 1$ , decreased monotonously with  $\alpha_s$ . This conclusion was shown to be supported by the data of numerical computations on nonintersecting random walks on three-dimensional lattices. An empirical equation of  $z$  was suggested as a function of  $\alpha_s$ , which yielded a constant value of  $1.28 \times 10^{-3}$  for  $z/M^{1/2}$  for the present polystyrene-toluene system regardless of molecular weight.

## I. Introduction

For flexible macromolecules perturbed by the excluded-volume effect, the mean-square radius of gyration  $\langle S^2 \rangle$  is not proportional to molecular weight  $M$  but to  $M$  to a power greater than unity. To avoid confusion, let us first define the parameter  $\gamma$  for this property as

$$\gamma = d \ln \langle S^2 \rangle / d \ln M \quad (1)$$

The perturbation may vanish at the theta temperature at which the second virial coefficient  $A_2$  becomes zero. Of experimentally observable quantities, most directly related to the excluded-volume effect is the expansion factor,<sup>3</sup> which is denoted as  $\alpha_s$  and defined by the ratio of  $\langle S^2 \rangle^{1/2}$  to its unperturbed value  $\langle S^2 \rangle_0^{1/2}$ .

Considerable experimental effort has been directed toward elucidating this effect since Flory introduced this concept in 1949,<sup>4</sup> but for the last 5 years essentially no work was published. This never means that the effect has been analyzed in so much detail that the expansion factor is uniquely and universally related to the parameter

$$z = (3/2\pi a^2)^{3/2} \beta n^{1/2} \quad (2)$$

as the theory predicts.<sup>5</sup> Indeed, Yamakawa undeniably described in a recent review<sup>6</sup> that "as for the detailed deductions and conclusions about this effect, there is not as yet a complete consensus of all polymer physical chemists and physicists". In experimental studies difficulty lay in the lack of accuracy despite the fact that important improvements were made.<sup>7,23</sup>

However, there are now sufficient reasons to believe that we can obtain more accurate light-scattering data. (1) There is available an improved light-scattering photometer.<sup>8</sup> The reduced scattered intensity on dilute polymer solutions can routinely be determined correct to 0.5–1.0% over the range of the scattering angle from 9 to 150°. Both the geometrical correction and the correction for the Fresnel reflection can be ignored. Quick temperature equilibration of the sample liquid, as well as the accurate temperature control, is possible. The stray light level is low enough to obtain the correct angular dependence of the scattering from benzene to 20°. It should be mentioned that the quality of light-scattering data can be

objectively evaluated on the results on pure liquids.<sup>9</sup> (2) Polymer samples of very high molecular weights with reasonably narrow molecular weight distribution can be prepared.<sup>10</sup> It has also been established on polystyrene<sup>7</sup> that the unperturbed mean-square radius of gyration varies linearly with molecular weight and depends on solvent conditions only slightly.<sup>11</sup> (3) We can evaluate both the second virial coefficient and the mean-square radius of gyration from the slopes of linear plots of directly measurable quantities. The present investigation has established the linear dependence on concentration of the square root of the reciprocal scattered intensity function provided that polymer concentration is sufficiently low (see below). For the evaluation of  $\langle S^2 \rangle$  we can make use of the Fujita plot.<sup>12</sup> The assumption of the Debye scattering function in Fujita's method was quantitatively examined both experimentally and theoretically by the present authors,<sup>15</sup> and the usefulness of the plot has thus been fully established.

In the present work we measured light scattering and viscosity on five polystyrene samples in toluene at 30 °C. Viscosity measurements were also made in *trans*-decalin at 20.4 °C (the theta temperature). To eliminate ambiguity in the final conclusion, emphasis was placed on making repeated measurements on a restricted number of samples rather than performing a single measurement each on more samples. The sample molecular weight ranged from 1.3 to 15.9 million. Three striking and unexpected observations were: (1) Double logarithmic plots of  $(\langle S^2 \rangle / M)$  against  $M$  gave a curve concave downward. (2) The corresponding quantity involved in viscosity, i.e.,  $([\eta] / [\eta]_0)$ , showed similar behavior. (3) The penetration function  $\Psi$  in the expression of  $A_2$  decreased with  $\alpha$  and tended to level off.

The direct deduction of the dependence of  $\alpha$  on  $z$  from experimental data of  $\langle S^2 \rangle$  and  $M$  has been difficult due to the fact that the absolute value of  $z$  cannot be determined by any experiment. But the problem was circumvented in the present investigation by unambiguously estimating the slope  $F$  in the double logarithmic plot of  $(\alpha^3 - 1)$  against  $M^{1/2}$ . It was concluded that  $F$ , being unity at  $\alpha = 1$ , decreased with  $\alpha$ . We reanalyzed the results of numerical studies on nonintersecting random walks on various lattices and found the data conformable to the above conclusion.

## II. Experimental Section

**Materials.** Polystyrenes were a gift of Dr. T. Hashimoto of Toyo Soda Manufacturing Co. The sample preparations and the molecular weight distributions estimated by gel-permeation chromatography were reported elsewhere.<sup>10</sup> The same sample codes as in the original report are used here: FF-8, FF-33, FF-35, FF-36, and FF-37. Reagent-grade toluene (Nakarai Chemicals, Kyoto) was purified as usual and fractionally distilled in a column just prior to use. Reagent-grade *trans*-decalin (Nakarai Chemicals, Kyoto) was passed through a column of silica gel and distilled under argon just before use. The boiling point of the collected fractions was 70.0–71.3 °C (20 mm). The purity of the *trans*-decalin thus prepared was checked on gas chromatograms as 99% pure. The refractive indices for the sodium H line were 1.49415 for toluene at 25 °C and 1.46927 for *trans*-decalin at 20 °C. These values are in good agreement with the respective literature values of 1.49413<sup>13</sup> and 1.46932.<sup>14</sup>

**Light-Scattering Measurements.** The light-scattering instrument used and the procedure employed in the present study were described in detail elsewhere.<sup>8,15</sup> Toluene was used as solvent and light scattering was measured at 30 °C with the vertically polarized incident beam of wavelength 435.8 nm. We measured as our routine experimental procedure the anisotropic light scattering, too, in order to always check the proper alignment of the optical system. Both pieces of data were processed in a desk computer by using a program. The reduced scattered intensity, denoted as  $R(\theta)$ , was thus corrected for the effect of optical anisotropy, but we do not mean that the correction was necessary. The refractive index of toluene was determined for the wavelength of incident beam as 1.512, and for the specific refractive index increment a value of 0.1134 was used.<sup>16</sup> The polymer concentration was determined of a dust-free solution of appropriate con-

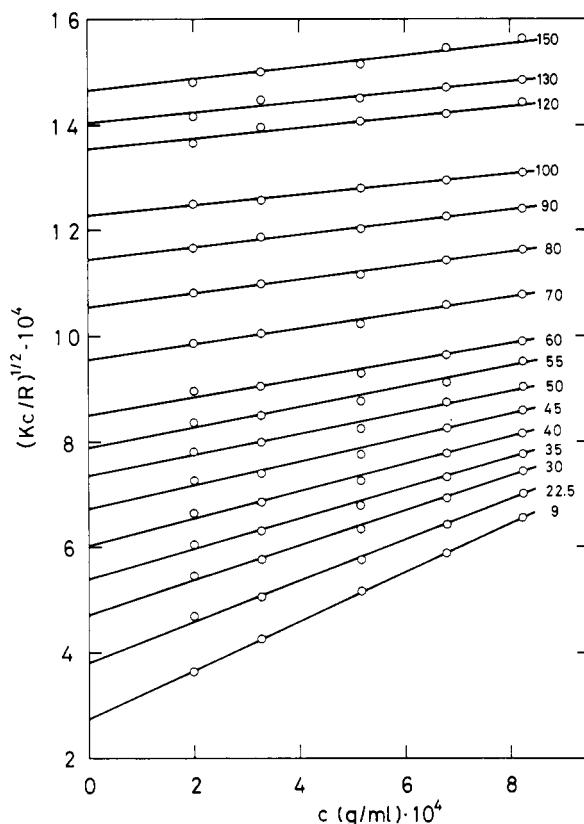


Figure 1. The linear concentration dependence of  $(Kc/R)^{1/2}$  on FF-37 in toluene at 30 °C. The scattering angle is indicated with each straight line.

centration by dry weight analysis using 0.8577 for the density of toluene at 30 °C.<sup>13</sup> Test solutions of desired concentration were individually prepared by mixing by weight the solution and the clean solvent. On the samples FF-8, FF-35, and FF-37, the measurement of  $\langle S^2 \rangle$  was independently repeated twice. It does not require the absolute concentration whose determination is quite time consuming. It may be pointed out that for polymers of very large molecular weight the scattered intensity is quite reduced at high angles due to the strong destructive interference. The second virial coefficient also becomes small. Therefore, in order to maintain the experimental accuracy in the determination of  $\langle S^2 \rangle$  and  $A_2$ , we should study a wider and higher concentration range than we usually use.<sup>15</sup>

**Viscosity Measurements.** Ordinary capillary viscometers of the Ubbelohde type were used for the measurements in *trans*-decalin at 20.4 °C (the theta temperature for the system). Kinetic energy corrections were found negligible, and the average shear stress did not exceed 7.3 dyn/cm<sup>2</sup>. We measured the viscosity in toluene in a rotating cylinder viscometer, which is a modification of a design suggested by Zimm and Crothers.<sup>17</sup> Its construction and use were described in detail elsewhere.<sup>18</sup> Relative viscosities measured at four values of average shear stress in the range 0.04–0.4 dyn/cm<sup>2</sup> were found essentially constant.

## III. Experimental Results

**Dependence of Light-Scattering Data on Concentration and Evaluation of  $A_2$ .** Figure 1 shows the concentration dependence of  $(Kc/R)^{1/2}$  on FF-37, the sample of the largest molecular weight examined here. The plotted points fall on a straight line at all the scattering angles. If we more closely examine the data, the points may appear to skew upwards in the angular range from 22.5 to 60°. However, this type of deviation from the straight line did not occur in a systematic way in the plots of other samples as we can judge from the values in Table I. The table also shows that the relative root-mean-square deviation of experimental data from the straight line drawn by the least-squares fit never exceeded 1%. Figure 2 shows the data extrapolated to zero scattering angle. The results mean that in the series expansion

**Table I**  
The Relative Root-Mean-Square Deviation (%) at Each Scattering Angle of the Experimental Data from the Straight Line<sup>a</sup> Drawn in the Plot of  $(Kc/R)^{1/2}$  vs. Concentration

	FF-8	FF-33	FF-35	FF-36	FF-37
Range of $c, \text{g/mL} \times 10^4$	1.7	1.8	1.5	1.7	2.0
Scattering angle, deg					
0	0.31	0.26	0.21	0.20	0.23
9		0.71	0.33	0.66	0.30
10		0.36	0.42	0.43	0.19
12	0.89	0.33	0.27	0.49	0.36
14.5	0.57	0.68	0.36	0.40	0.46
17	0.51	0.34	0.42	0.24	0.42
19.5	0.21	0.38	0.22	0.20	0.68
22.5	0.50	0.34	0.28	0.19	0.62
26	0.42	0.41	0.35	0.37	0.75
30	0.44	0.30	0.32	0.38	0.79
35	0.66	0.39	0.36	0.39	0.69
40	0.66	0.31	0.43	0.36	0.84
45	0.26	0.11	0.48	0.40	0.87
50	0.48	0.22	0.49	0.47	0.90
55	0.42	0.30	0.31	0.49	0.84
60	0.57	0.43	0.48	0.53	0.61
70	0.38	0.65	0.37	0.49	0.41
80	0.68	0.63	0.53	0.29	0.22
90		0.36	0.64	0.39	0.21
100	0.54	0.60	0.75	0.26	0.12
110		0.44	0.54	0.61	
120	0.53	0.65	0.73	0.11	0.41
130	0.71	0.68	0.63	0.28	0.43
150	0.66	0.67	0.68	0.40	0.21

<sup>a</sup> The straight line was determined by the least-squares fit to the data.

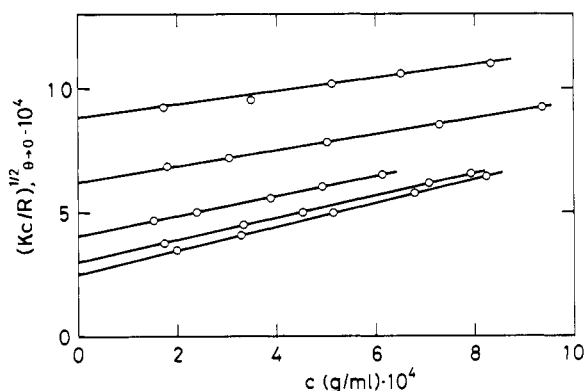


**Figure 2.** The linear concentration dependence of  $(Kc/R)^{1/2}_{\theta=0}$  in toluene at 30 °C for the samples (from the top) FF-8, FF-33, FF-35, FF-36, and FF-37.

$$(KcM/R)^{1/2}_{\theta=0} = 1 + A_2Mc + (3A_3 - A_2^2M)(M/2)c^2 + \dots \quad (3)$$

we can neglect higher terms than the second under the present experimental condition. The second virial coefficient and the molecular weight estimated from the slope and the intercept, respectively, are summarized in Table II.<sup>19</sup>

**Dependence of Light-Scattering Data on Angle and Evaluation of  $\langle S^2 \rangle$ .** Figure 3 shows the square-root plots of the light-scattering results extrapolated to zero solute concentration, where, for the clear representation, the data for the scattering angles greater than 70° were omitted and the

**Table II**  
Light-Scattering and Viscosity Data for Polystyrene Samples of High Molecular Weights

	FF-8	FF-33	FF-35	FF-36	FF-37
Light-Scattering Data					
$M \times 10^{-6}$	1.29	2.58	6.12	11.1	15.9
$\langle S^2 \rangle \times 10^{11}, \text{cm}^2$	2.37	5.62	16.1	31.7	47.7
	(2.35) <sup>a</sup>		(15.9)		(47.3)
$A_2 \times 10^4, \text{mol mL g}^{-2}$	2.35	1.99	1.64	1.34	1.21
Viscosity Data <sup>b</sup>					
$[\eta], \text{dL/g (trans-decalin)}$	0.87	1.25	1.91	2.72	3.46
$[\eta], \text{dL/g (toluene)}$	2.80	4.78	9.22	14.29	19.97

<sup>a</sup> Results obtained by the separate measurements. <sup>b</sup> Measurements were made at 30.0 °C in toluene and at 20.4 °C (the  $\theta$  temperature) in *trans*-decalin.

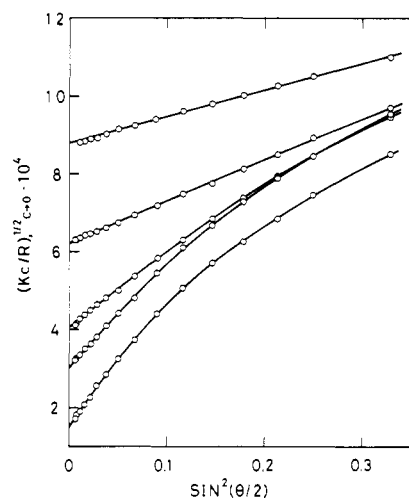


**Figure 3.** Square-root plots of the light-scattering data extrapolated to zero solute concentration on the samples (from the top) FF-8, FF-33, FF-35, FF-36, and FF-37. The data for FF-37 were plotted downward by one unit.

data points for FF-37 were displaced by one unit downward. In this angular range the data for the samples of low molecular weights, i.e., FF-8 and FF-33, fall on straight lines, whereas the plotted points for other samples show marked downward curvature, which makes the unambiguous estimate of  $\langle S^2 \rangle$  difficult or impossible. Unfortunately such an ambiguity was involved in some data which had been published before a useful relation was worked out by Fujita in 1970.<sup>12</sup> The relation reads

$$y = M^{-1} + bZ(u) \quad (4)$$

where

$$y = \lim_{c \rightarrow 0} \frac{Kc}{R(\theta)} \quad (5)$$

$$u = \sin^2(\theta/2), \quad b = (32\pi^2/3\lambda^3)(\langle S^2 \rangle/M) \quad (6)$$

and

$$Z(u) = yu^{-4/3} \int_0^u y^{-1}(u)u \, du \quad (7)$$

The numerical integration in eq 7 was performed using Simpson's formula. The results obtained are shown in Figure 4. Some scattering of points at small  $Z$  apparently indicates a larger experimental error in  $R$  for very small scattering angles due to the difficulty in keeping the residual dust in test solutions and solvents at a constant level. Fortunately, how-

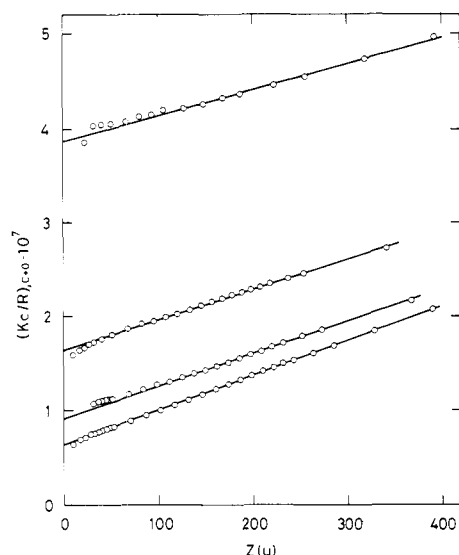


Figure 4. Fujita's plots for the samples (from the top) FF-33, FF-35, FF-36, and FF-37 in the range of small scattering angles. A similar plot for the entire angular range is shown in Figure 18.

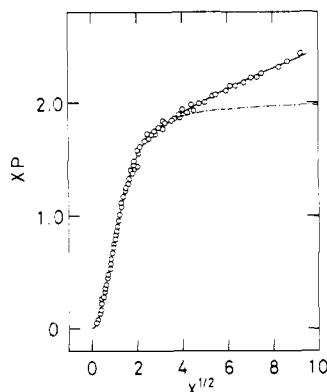


Figure 5. The particle scattering factor  $P$  as a plot of  $xP(x)$  vs.  $x$  [ $= \langle S^2 \rangle (4\pi/\lambda)^2 \sin^2(\theta/2)$ ] on polystyrene samples in toluene at 30 °C. The chain curve represents the Debye equation and the thick curve eq 20 in ref 15 with  $\epsilon = 0.175$  and  $l = 2.85$ .

ever, the increased error in  $R$  for very small scattering angles does not affect at all the accuracy in the determination of  $Z$  at higher angles. In addition, since the range of linear dependence in the plot of  $y$  vs.  $Z(u)$  is quite wide, the initial straight line can be drawn unambiguously. Furthermore, the intercepts so obtained agreed with those determined in Figure 2 within the experimental error. The values of  $\langle S^2 \rangle$  estimated from the slopes are summarized in Table II. Duplicate and independent determinations of  $\langle S^2 \rangle$  on three samples (data in parentheses) yielded the results in agreement within 2% with one another.

The Fujita method is based on the experimental result<sup>15</sup> that the particle scattering factor  $P$  for linear flexible polymers in dilute solution can in general be approximated by the well-known Debye equation unless the value of the parameter  $x$  [ $= \langle S^2 \rangle (4\pi/\lambda)^2 \sin^2(\theta/2)$ ] exceeds about 10. This result was verified again by the present experimental data as shown in Figure 5.

**Viscosity Data and Evaluation of  $[\eta]$ .** Figure 6 shows the viscosity data in toluene at 30.0 °C measured in the rotating cylinder viscometer with a rate of revolution of the outer magnet of 40 rpm. Both the Fuoss-Mead plot ( $\ln \eta_{rel}/c$  vs.  $c$ ) and the Schulz-Blaschke plot ( $\eta_{sp}/c$  vs.  $\eta_{sp}$ ) gave the straight lines with the identical intercept, while the plotted points were

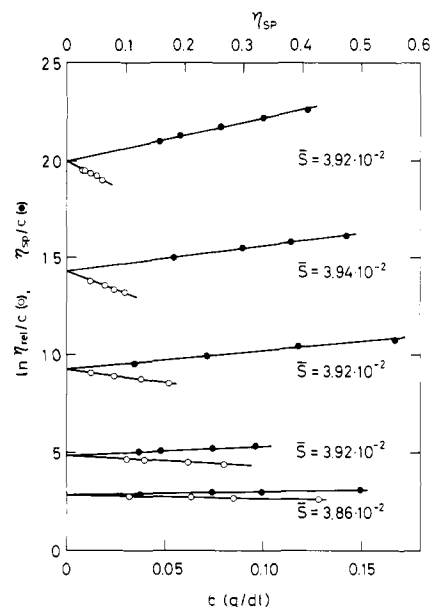


Figure 6. The Fuoss-Mead plot ( $\ln \eta_{rel}/c$  vs.  $c$ , open circles) and the Schulz-Blaschke plot ( $\eta_{sp}/c$  vs.  $\eta_{sp}$ , closed circles) of viscosity data in toluene at 30 °C measured in the rotating-cylinder viscometer. The samples are from the top FF-37, FF-36, FF-35, FF-33, and FF-8. The average shear stress (dyn/cm<sup>2</sup>) used is indicated.

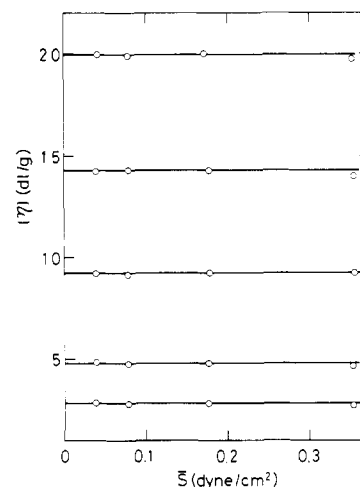
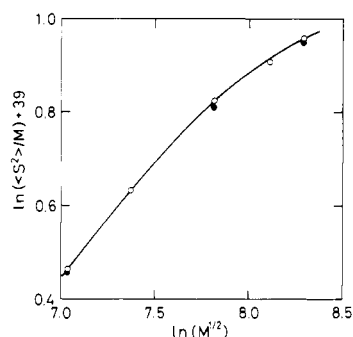


Figure 7. The dependence of  $[\eta]$  (toluene, 30 °C) on the average shear stress on the samples (from the top) FF-37, FF-36, FF-35, FF-33, and FF-8.

curved in the Huggins plot. As shown in Figure 7 the results of  $[\eta]$  exhibit no dependence on shear stress in the range examined here. The measurements with capillary viscometers yielded the smaller values of  $[\eta]$  except for FF-8, and the difference increased with molecular weight. The data of  $[\eta]$  in toluene, as well as those in *trans*-decalin, are summarized in Table II.

#### IV. Discussion

**Chain Expansion Factor.** The current theory predicts that the expansion factor  $\alpha$  is a single-valued function of  $z$ .<sup>5</sup> The parameter  $z$  should vary linearly with  $M^{1/2}$ , but the proportionality constant cannot be determined by separate experiments. This has been the inherent difficulty in the data analysis and hence the source of great confusion. For example, Berry<sup>7</sup> estimated  $\psi$  by assuming its temperature dependence as  $(1 - \theta/T)$ , but the assumption was later criticized as invalid.<sup>5</sup>



**Figure 8.** Double logarithmic plots of  $\langle S^2 \rangle / M$  vs.  $M^{1/2}$  for polystyrene in toluene at 30 °C. The closed circles show the plots for  $\langle S^2 \rangle$  determined by separate experiments.

Here we start from the basic two assumptions: (1)  $\langle S^2 \rangle_0$  is proportional to molecular weight. (2) The parameter  $z$  is proportional to  $M^{1/2}$ . It is then straightforward that we can study the power-law dependence of  $\alpha^2$  on  $z$  from the double logarithmic plot of  $(\langle S^2 \rangle / M)$  against  $M^{1/2}$ . Quite unexpectedly, the plotted points exhibit a downward curvature as shown in Figure 8; all the existing theories predict the opposite curvature.<sup>5</sup> We proceed to further analyze the dependence in terms of  $F$  as defined by

$$F = d \ln (\alpha^3 - 1) / d \ln z \quad (8)$$

with  $F = 1$  at  $\alpha = 1$  (assumption 3). Since the data points in Figure 8 fall on a very smooth curve,<sup>20</sup> we may unambiguously determine the value of  $F$  as a function of  $\alpha$  by plotting  $(\alpha^3 - 1)^n / M^{1/2}$  against  $\alpha$ , where  $n$  is a constant. The  $\alpha$  value was calculated using  $10^{18} \langle S^2 \rangle_0 / M = 7.6$ .<sup>7,19</sup> The results are shown in Figure 9, where for each  $n$  the ordinate values are divided by the value for FF-8 and the abscissa values are displaced by  $n$  for the clear representation. The  $n$  value chosen gives  $F^{-1}$  corresponding to the  $\alpha$  value at the maximum of each curve. The retention of the smoothness of the resulting plot for  $n$  values up to 2.4 assures the accurate estimate of  $F$ . In addition the smooth and asymptotic reach to unity of the data points for  $n = 1$  with decrease in  $\alpha$  may be regarded as indicating the appropriate choice of eq 8 or the validity of assumption 3.

Figure 10 shows the results of  $F$  so determined as a function of  $(\alpha - 1)$ . As expected from the downward curvature in Figure 8 the  $F$  value is seen to decrease rapidly with  $\alpha$  in the range 1.5–2.0. We know nothing about the dependence beyond this range, but it is unnatural to consider a negative  $F$  value. In any case, we found that the dependence of  $F$  on  $(\alpha - 1)$  obtained by the experiment could be closely approximated by (assumption 4)

$$F^{-1} = 1 + \exp[a(\alpha - 1) - b] \quad (9)$$

where  $a$  and  $b$  are numerical constants. This is the Fermi function in quantum statistics and the curve in Figure 10 was drawn with  $a = 9.9$  and  $b = 9.2$ . Using this result in

$$F = \frac{d \ln (\alpha^3 - 1)}{d \ln z} = \frac{3\alpha^2 z}{(\alpha^3 - 1)} \frac{d\alpha}{dz} \quad (10)$$

we obtain a function relating  $z$  to  $\alpha$  by separating the variable and repeating the integration by parts on  $\alpha$ . One may feel that the analysis is advanced too far beyond a legitimate limit, but the result is useful at least for checking the internal consistency that the  $z$  value computed from  $\alpha$  by the equation is proportional to  $M^{1/2}$  (assumption 2). If this obtains, the evaluation of  $F$  as in Figure 9 may be regarded as correct, too. The result reads

$$\ln z = \ln (2/3C_1) + \ln (\alpha^3 - 1) + \frac{3}{a(\alpha^3 - 1)} \exp[a(\alpha - 1) - b] G(\alpha) \quad (11)$$

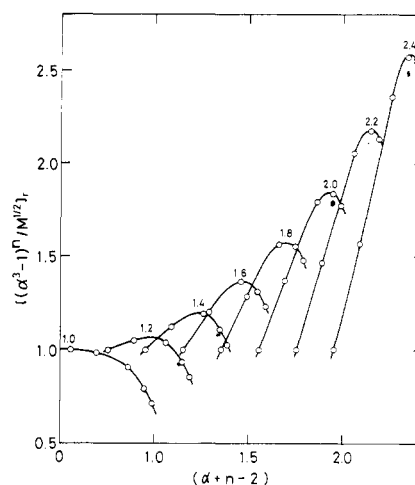


**Figure 9.** The determination of  $F$  in eq 8 as a function of  $\alpha$  (see text). The number  $n$  chosen is indicated with each curve.

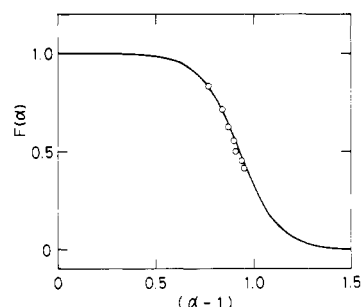


**Figure 10.** The dependence of  $F$  in eq 8 on  $(\alpha - 1)$  on the data of polystyrene in toluene at 30 °C. The curve shows eq 9 with  $a = 9.9$  and  $b = 9.2$ .

with

$$G(\alpha) = \alpha^2 + \frac{\alpha^4 + 2\alpha}{a(\alpha^3 - 1)} + \frac{2(\alpha^6 + 7\alpha^3 + 1)}{[a(\alpha^3 - 1)]^2} + \frac{6(\alpha^8 + 16\alpha^5 + 10\alpha^2)}{[a(\alpha^3 - 1)]^3} + \frac{24(\alpha^{10} + 30\alpha^7 + 45\alpha^4 + 5\alpha)}{[a(\alpha^3 - 1)]^4} + \dots \quad (12)$$

The convergence of the series in eq 12 is good and higher terms are not necessary for the present purpose. The numerical constant  $C_1 (=1.276)$  was chosen so as to fit the perturbation theory. The numerical results of  $z$  calculated from  $\alpha$  according to eq 11 are summarized in Table III. The perfect constancy of the ratio  $(z/M^{1/2})$  obtained therefore verifies, though indirectly, that assumptions 3 and 4 are valid.

The dependence of the chain expansion factor  $\alpha$  on molecular weight is usually discussed in terms of  $\gamma$  in eq 1. It should be pointed out, however, that the conventional double logarithmic plot of  $\langle S^2 \rangle$  against  $M$  gives no useful information because the net effect of the excluded volume appears only in the small number of  $\gamma - 1$ . Here we determine  $\gamma$  by calculation from  $F$  by the relation

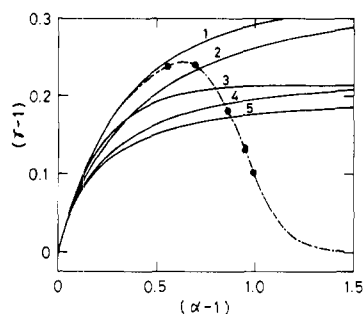
$$\gamma = \frac{d \ln \langle S^2 \rangle}{d \ln M} = 1 + \frac{F(\alpha^3 - 1)}{3\alpha^3} \quad (13)$$

Figure 11 shows the results as a function of  $\alpha$ . The maximum value to be attained may depend on assumption 3.

**Penetration Function  $\Psi$ .** The dependence of  $\langle S^2 \rangle$  on molecular weight obtained in this study presents a sharp

**Table III**  
The Results of  $z$  Calculated by Equation 11 from  $\alpha$  and the Constancy of  $(z/M^{1/2})$  Regardless of Molecular Weight

	$M^{1/2} \times 10^{-3}$	$\alpha$	$z$	$(z/M^{1/2}) \times 10^3$
FF-8	1.13 <sub>5</sub>	1.56	1.45	1.28
FF-33	1.60 <sub>7</sub>	1.69	2.06	1.28
FF-35	2.47 <sub>3</sub>	1.86	3.18	1.29
FF-36	3.32 <sub>7</sub>	1.95	4.25	1.28
FF-37	3.98 <sub>2</sub>	1.99	5.09	1.28



**Figure 11.** The power-law dependence of  $\langle S^2 \rangle$  on  $M$  (eq 1) as a plot of  $(\gamma - 1)$  vs.  $(\alpha - 1)$ . The chain curve represents eq 13 with use of eq 9 for  $F$ , and closed circles show the values for the samples studied here. Other curves represent some existing approximate theories:<sup>5</sup> (1) Fixman equation; (2) Ptitsyn equation; (3) Kurata-Alexandrowicz equation; (4) Yamakawa-Tanaka equation; (5) Flory equation.

contrast with the present understanding of the behavior of polymer chains perturbed by the excluded-volume effect. No interpretation is given here for the new result, but it seems to suggest that when the molecular weight becomes exceedingly large the intramolecular energy due to the effect can be relaxed by a conformation whose gyration radius is increasingly less than that expected from eq 1 with constant  $\gamma$ . In addition, we may well expect that the intermolecular interaction will reveal the consistent behavior via the penetration function  $\Psi$  in the expression of  $A_2$

$$A_2 = 4\pi^{3/2}N_A(\langle S^2 \rangle^{3/2}/M^2)\Psi \quad (14)$$

Figure 12 shows the plot of the experimental data of  $\Psi$  vs.  $\alpha^3$ . In agreement with the above expectation the  $\Psi$  values decrease with  $\alpha$  (or  $M$ ) and asymptotically reach a constant value, ca. 0.21.

**Limiting Viscosity Number.** The viscosity plot analogous to Figure 8 also gives a curve concave downward as shown in Figure 13. A still clearer confirmation of the curvature is given by the linear dependence in the double logarithmic plot of  $[\eta]/[\eta]_0$  vs.  $\alpha^3$  (Figure 14). A straight line can be drawn to pass through the origin. This result also indicates that the relation  $[\eta] = [\eta]_0\alpha^k$  ( $k = \text{constant}$ ) obtains not only near the theta solvent condition<sup>24</sup> but in good solvent systems. The  $k$  value was evaluated from the slope as 2.38. Unfortunately, however, we cannot conclude these without reservation, because the data of  $10^4[\eta]_0/M^{1/2}$  for FF-36 and FF-37 were persistently obtained larger than the average of the data for other samples (8.19 for FF-36 and 8.70 for FF-37 as compared to 7.72). The reason for the discrepancy is still unknown; the data of  $\langle S^2 \rangle_0/M$  for these samples showed no anomaly.<sup>19</sup>

**Reconsideration of the Results of Numerical Computations on Lattices.** Here we analyze the results of numerical computations on three-dimensional lattices to examine if they conform to the conclusion drawn above from the light-scattering data. Figure 15 shows the double logarithmic plot of  $\alpha_R^2$  against  $N^{1/2}$ , where  $\alpha_R$  is the expansion factor for the end-

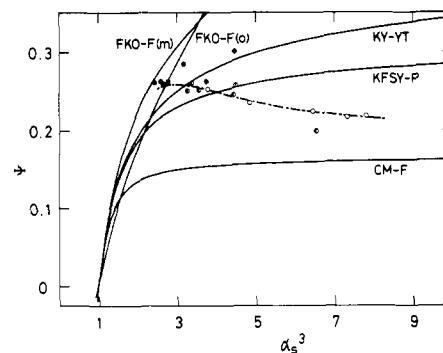


**Figure 12.** Plots of experimental data of  $\Psi$  vs.  $\alpha^3$  (open circles). Some existing data are plotted together: (●) Berry;<sup>7</sup> (○) Yamamoto et al.;<sup>21</sup> (●) Baumann.<sup>22</sup> The curve represents the relation calculated by the conjugate pair of theories.<sup>5</sup>

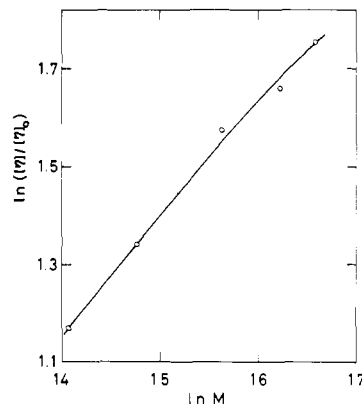


**Figure 13.** Double logarithmic plots of  $[\eta]/[\eta]_0$  vs.  $M$  on polystyrene in toluene at 30 °C.

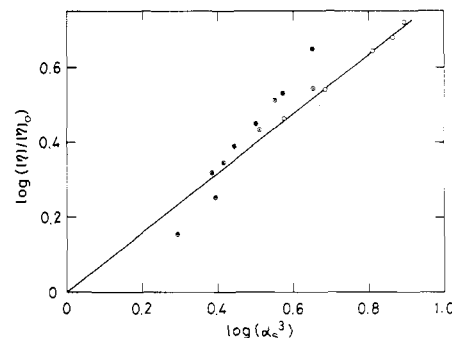


**Figure 14.** Double logarithmic plots of  $[\eta]/[\eta]_0$  vs.  $\alpha^3$  on polystyrene in toluene at 30 °C (open circles). Some existing data are plotted together: (●) Berry;<sup>7</sup> (○) Yamamoto et al.;<sup>21</sup> (●) Serdyuk and Grenader.<sup>23</sup>

to-end distance and  $N$  is the number of bonds. For the tetrahedral lattice and the five-choice simple cubic lattice, the exact enumeration data and the Monte-Carlo data are plotted together. In both cases the two sets of data lie on a single composite curve, and the slope, as concluded separately in the original papers, asymptotically approaches 0.4 ( $\alpha^5 \propto N^{1/2}$ ) for short chains and decreases below this value for longer chains. A similar plot is shown in Figure 16 for  $\alpha_s$ . Of special interest are the data of Suzuki,<sup>30</sup> which were obtained on the tetrahedral lattice using a dimerization technique. In the region of large  $N$  the data clearly show a downward curvature. Suzuki concluded, in perfect agreement with our data, that "with the increase in  $N$ ,  $\gamma$  increases at first but gradually decreases after

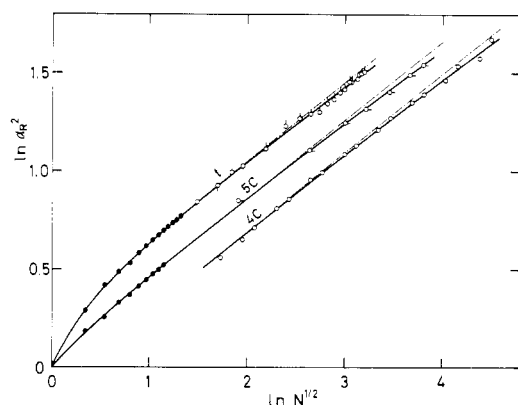


**Figure 15.** Double logarithmic plots of  $\alpha_R^2$  vs.  $N^{1/2}$ , where  $\alpha_R$  is the expansion factor for the end-to-end distance and  $N$  is the number of bonds. Symbols on curves mean the following: t, tetrahedral lattice; 5C, five-choice simple cubic lattice; 4C, four-choice simple cubic lattice. The data were taken from: (●) Domb;<sup>25</sup> (○) Wall and Erpenbeck;<sup>26</sup> (○) Wall and Whittington;<sup>27</sup> (○) Kron and Ptitsyn;<sup>28</sup> (○) Alexandrowicz.<sup>29</sup> The straight chain lines are drawn with the slope of 0.4.

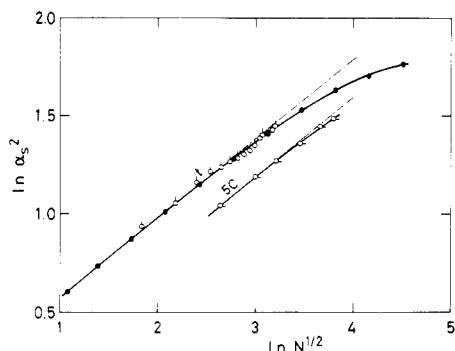


**Figure 16.** Double logarithmic plots of  $\alpha_s^2$  vs.  $N^{1/2}$ . For the symbols see the legend to Figure 15. The data were taken from: (●) Suzuki;<sup>30</sup> (○) Wall and Erpenbeck;<sup>26</sup> (○) Kron and Ptitsyn.<sup>28</sup>

passing a maximum value, 1.20", and that "it probably approaches unity very slowly". We analyzed his data according to eq 8 and found the decrease in  $F$  with  $\alpha$ . The  $\alpha$  value at  $F = 0.5$  was 2.2, as compared to 1.9 for the system polystyrene-toluene.

**Criticism to the Conventional Analysis of Light-Scattering Data.** In testing the validity of closed expressions for  $\alpha(z)$  and  $\Psi(z)$  by using light-scattering data, the judgment was often based on the following criteria:<sup>5</sup> (1) The values of  $z$  calculated by a theoretical equation for  $\alpha(z)$  from the measured  $\alpha$  values vary linearly with  $M^{1/2}$ . (2) When the experimental data of  $\alpha$  are plotted against the corresponding experimental data of  $\Psi$ , the data points form a single composite curve, and the chosen theory of  $\alpha$  and its conjugate theory of  $\Psi$  describe the composite curve correctly. We discuss the first criterion here. It by no means looks inappropriate, but nevertheless we can show that the correct judgment requires the proper estimate of the experimental error in  $z$  so determined. Figure 17 shows as an example the plot of  $z$  values calculated from the present light-scattering data by the Yamakawa-Tanaka theory.<sup>31</sup> If we simply regard the deviations of the data points from the straight line as the experimental error, one may erroneously conclude that the criterion is satisfied. However, the dotted curve in the figure should be the true dependence. The present example therefore suggests that the experimental data should be analyzed first on the basis of

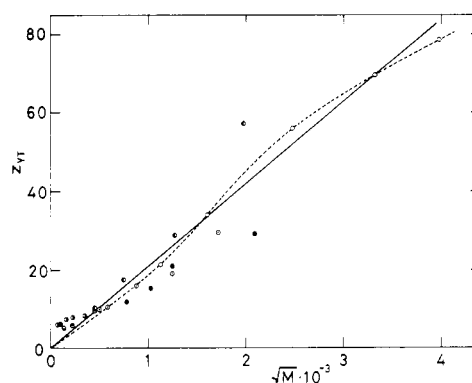


**Figure 17.** Plots against  $M^{1/2}$  of  $z$  values calculated by the Yamakawa-Tanaka equation<sup>31</sup> from the data of the present work (open circles). Some existing data are plotted together: (●) Berry;<sup>7</sup> (○) Yamamoto et al.;<sup>21</sup> (●) Baumann;<sup>22</sup> (●) Kirste and Wild;<sup>22</sup> (●) Serdyuk and Grenader;<sup>23</sup> (●) Wada et al.<sup>32</sup>

more fundamental properties such as the power-law dependence of  $\langle S^2 \rangle / M$  on  $M^{1/2}$ .

**Effects of Possible Uncertainties in the Determinations of  $\langle S^2 \rangle$  and  $M$ .** The most important finding of the present investigation is the dependence on molecular weight of the expansion factor in the way as shown in Figure 8. This result is also most unexpected, and we need therefore to fully explore the results of any reasonable uncertainties in the determinations of  $\langle S^2 \rangle$  and  $M$ .

First we examine the effect of convergence of rays in the incident beam. In the light-scattering photometer used,<sup>8</sup> an achromatic lens of a focal length of 74.8 mm forms the image of the aperture stop at the center of the measuring cell. A field stop located just behind the lens is 15 mm (vertically) by 10 mm (horizontally) and the beam size at the cell center is 3.1 mm (vertically) by 1.6 mm (horizontally). We take now a  $X$ - $Y$  rectangular coordinate system with the  $X$  axis in the horizontal direction. The beam axis passes through the origin. We take another similar  $x$ - $y$  coordinate system at the cell center and consider the rays which leave the field stop at an area element of  $dX dY$  at the point  $(X, Y)$  and reach the cell center at an element of  $dx dy$  at the point  $(x, y)$ . The angle  $\theta'$  that the rays form with the direction of the receiving optical system is given by

$$\cos \theta' = \cos \theta - \frac{x - X}{L} \sin \theta \quad (15)$$

where  $\theta$  is the scattering angle and  $L$  is the distance between the lens and the cell center (ca. 230 mm when the bath liquid is not used). This equation gives

$$\sin^2 (\theta'/2) = \sin^2 (\theta/2) + \frac{x - X}{2L} \sin \theta \quad (16)$$

Since the reduced scattered intensity is given as the first approximation by  $R = A - B \sin^2 (\theta'/2)$  ( $A$  and  $B$  are constants), we sum  $R$  for all the rays in the incident beam by using eq 16. The result shows that the effect of convergence of the incident rays vanishes due to the symmetry nature of the beam.

Next we consider the Fujita method of estimating  $\langle S^2 \rangle$  and  $M$  from light-scattering data. This method is based on the Debye scattering function that can be applied only to polymers in the theta solution. Therefore, we need to explore the effects of inadequacies of this function in good solvent systems on the estimates of  $\langle S^2 \rangle$  and  $M$ . Table IV compares the data of  $\langle S^2 \rangle$  estimated from the Fujita plot and those from the square-root plot. The table also shows the angular range where the data vary linearly in the square-root plot. The capability of our light-scattering apparatus of accurately measuring the

**Table IV**  
Comparison of  $\langle S^2 \rangle$  Data Estimated from the Fujita Plot and those from the Square-Root Plot and the Linear Range of Scattering Angles in the Latter Plot

	FF-8	FF-33	FF-35	FF-36	FF-37
	$\langle S^2 \rangle \times 10^{11}, \text{cm}^2$				
Fujita's plot	2.37	5.62	16.1	31.7	47.7
Square-root plot	2.37	5.46	15.5	29.7	45.2
Deviation, %	0	-2.5	-3.9	-6.7	-5.5
	Linear Range in the Square-Root Plot				
$\sin^2 (\theta/2)$	0-1	0-0.25	0-0.09	0-0.05	0-0.03
$\theta$ , deg	0-150	0-60	0-35	0-25	0-20

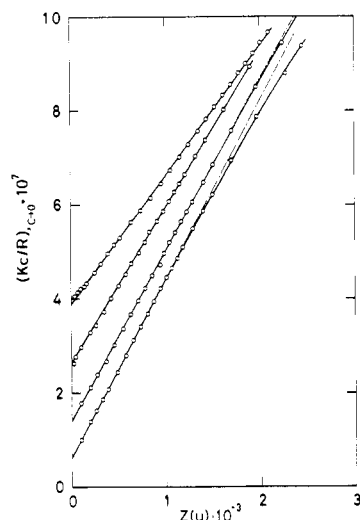


**Figure 18.** Fujita plots for the samples (from the top) FF-33, FF-35, FF-36, and FF-37 in the entire range of scattering angles. For the clear representation, the data for FF-35 are plotted upwards by one unit and those for FF-36 by half a unit.

reduced scattered intensity at small angles allows estimates of  $\langle S^2 \rangle$  for the samples FF-8 and FF-33 from the square-root plot. However, the linear angular range becomes so drastically limited at higher molecular weights that the error associated with the estimate of the limiting slope increases for FF-35, FF-36, and FF-37. In the Fujita plot, on the contrary, the data of FF-8, FF-33, and FF-35 fall strictly on straight lines over the entire range of scattering angles as shown in Figure 18 (the plots for FF-8 are not shown there, because it is self-evident that the data that are linear in the square-root plot are also linear in the Fujita plot). Even the data of FF-37 fall on a straight line up to an angle of  $50^\circ$ . These results clearly indicate that the effects of inadequacies of the Debye function appear only at high angles for samples with very large gyration radii. In other words, the particle scattering factor for polymers in good solvent systems deviates from the Debye function only for  $x = [(4\pi/\lambda)^2 \sin^2 (\theta/2) \langle S^2 \rangle]$  greater than 10 in agreement with the conclusion obtained in our earlier investigation.<sup>15</sup> We can quantitatively check this with the data on FF-37 as shown in Table V.

One more advantage of the Fujita plot is due to the fact that the abscissa value  $Z(u)$  is unaffected by the increased experimental error in  $R$  for very small angles; the integrand includes  $u$  which becomes very small at small angles, and the error in  $y^{-1}$  in the integrand is partially canceled by the factor of  $y$  outside of the integral. Thus the Fujita plot also helps in locating the intercept or estimating molecular weight.

Finally it should be mentioned that the result of Figure 8 is unaffected by the values of the calibration constant and the

**Table V**  
Comparison of the Particle Scattering Factor for FF-37 and the Debye Function at Various Scattering Angles

Angle $\theta$ , deg	$x$	$P(\text{exptl})$	$P, D$	Rel dev, %
9	0.559	0.846	0.837	1.1
10	0.690	0.783	0.805	-2.7
12	0.992	0.741	0.737	0.4
14.5	1.446	0.653	0.652	0.2
17	1.983	0.583	0.570	2.2
19.5	2.571	0.495	0.498	-0.7
22.5	3.455	0.419	0.417	0.6
26	4.594	0.345	0.342	1.1
30	6.081	0.278	0.275	1.3
35	8.209	0.212	0.214	-1.1
40	10.62	0.169	0.171	-0.8
45	13.29	0.138	0.139	-0.6
50	16.21	0.118	0.116	1.8
55	19.36	0.101	0.0980	3.1
60	22.70	0.0867	0.0842	2.9
70	29.87	0.0688	0.0647	6.4
80	37.51	0.0562	0.0519	8.2
90	45.39	0.0476	0.0431	10.4
100	53.27	0.0412	0.0368	11.8
120	68.09	0.0335	0.0289	15.7
130	74.57	0.0312	0.0264	17.8
150	84.70	0.0283	0.0233	21.1

specific refractive index increment. What we need are only the direct light-scattering data and the concentration.

In summary, we are unable to find, until now at least, any source of experimental error which seriously injures the conclusion in this investigation. Additional work at still higher molecular weight and similar careful light-scattering investigations at other institutions are required before the problem is settled.<sup>33</sup> Extension of the studying range to higher molecular weight is still difficult, however, because the wider distribution of molecular weight will cause the data to deviate upwards in Figure 8.

**Acknowledgment.** We are indebted to Dr. K. Suzuki for the discussion on the results for nonintersecting random walks on the tetrahedral lattice.

## References and Notes

- (1) Presented in part at the 26th IUPAC Congress, Tokyo, September 1977.
- (2) Address correspondence to this author at the Faculty of Integrated Arts and Sciences, Hiroshima University, Hiroshima 730, Japan.
- (3) Hereafter abbreviated as  $\alpha$  unless otherwise indicated.
- (4) P. J. Flory, "Principles of Polymer Chemistry", Cornell University Press, Ithaca, N.Y., 1953.
- (5) H. Yamakawa, "Modern Theory of Polymer Solutions", Harper and Row, New York, N.Y., 1971.
- (6) H. Yamakawa, *Annu. Rev. Phys. Chem.*, **25**, 186 (1974).
- (7) G. C. Berry, *J. Chem. Phys.*, **44**, 4550 (1966).
- (8) H. Utiyama and Y. Tsunashima, *Appl. Opt.*, **9**, 1330 (1970).
- (9) H. Utiyama in "Light Scattering from Polymer Solutions", M. Huglin, Ed., Academic Press, New York, N.Y., 1972, Chapter 4.
- (10) M. Fukuda, M. Fukutomi, Y. Kato, and T. Hashimoto, *Polym. J.*, **12**, 871 (1974).
- (11) For poly( $\alpha$ -methylstyrene) both of these conditions did not obtain. We cannot use such polymers for the study of excluded-volume effects. Y. Tsunashima, H. Utiyama, and M. Kurata, unpublished data.
- (12) H. Fujita, *Polym. J.*, **1**, 537 (1970).
- (13) J. A. Riddick and E. E. Toops, Ed., "Organic Solvents", Interscience, New York, N.Y., 1955.
- (14) D. L. Camin and F. D. Rossini, *J. Phys. Chem.*, **59**, 1173 (1955).
- (15) H. Utiyama, Y. Tsunashima, and M. Kurata, *J. Chem. Phys.*, **55**, 3133 (1971).
- (16) J. H. O'Mara and D. McIntyre, *J. Phys. Chem.*, **63**, 1435 (1959).
- (17) B. H. Zimm and D. M. Crothers, *Proc. Natl. Acad. Sci. U.S.A.*, **48**, 905 (1962).
- (18) N. Sugi, Y. Tsunashima, K. Ikehara, and H. Utiyama, *Jpn. J. Appl. Phys.*, **11**, 1547 (1972).



- (19) The data of molecular weight reported by Fukuda et al.<sup>10</sup> on the same samples are all smaller than the present data, and the difference increases with molecular weight. The discrepancy was found to originate from the error in their concentration determination. The solution on which the concentration had been determined was filtered through a Millipore filter, and the light-scattering measurements were carried out on the filtrate. Therefore, the concentration was overestimated due to the retention of some material on the filter. The higher the sample molecular weight becomes the larger is the amount of the retained material. Their data of  $A_2$  may also involve some error. The data of  $\langle S^2 \rangle$  may be least affected because the relative concentration suffices for the measurement. Indeed, reevaluation of  $10^{18} \langle S^2 \rangle / M$  (*trans*-decalin, 20.4 °C) with use of molecular weight obtained here yields a constant 7.28 irrespective of molecular weight within 3%. However, for the sake of clarity we used in the later analysis a value of 7.60 as reported by Berry.<sup>7</sup> A similar experimental procedure was employed for the concentration determination by Kato et al. on the study of poly( $\alpha$ -methylstyrene): T. Kato, K. Miyaso, I. Noda, T. Fujimoto, and M. Nagasawa, *Macromolecules*, **3**, 777 (1970).
- (20) As  $10^{11} \langle S^2 \rangle$  for FF-36 we used 31.9<sub>5</sub> instead of 31.7 in order to fit the data on the smooth curve in Figure 8.
- (21) A. Yamamoto, M. Fujii, G. Tanaka, and H. Yamakawa, *Polym. J.*, **2**, 799 (1971).
- (22) H. Baumann, cited in the paper by Kirste and Wild: R. G. Kirste and G. Wild, *Makromol. Chem.*, **121**, 174 (1969).
- (23) N. Serdyuk and K. Grenader, *Makromol. Chem.*, **175**, 1881 (1974).
- (24) M. Kurata and H. Yamakawa, *J. Chem. Phys.*, **29**, 311 (1958).
- (25) C. Domb, *J. Chem. Phys.*, **38**, 2957 (1963).
- (26) F. T. Wall and J. J. Erpenbeck, *J. Chem. Phys.*, **30**, 637 (1959).
- (27) F. T. Wall and S. G. Whittington, *J. Phys. Chem.*, **73**, 3953 (1969).
- (28) A. K. Kron and O. B. Ptitsyn, *Vysokomol. Soedin., Ser. A*, **9**, 759 (1967).
- (29) Z. Alexandrowicz, *J. Chem. Phys.*, **51**, 561 (1969).
- (30) K. Suzuki, *Bull. Chem. Soc. Jpn.*, **41**, 538 (1968).
- (31) H. Yamakawa and G. Tanaka, *J. Chem. Phys.*, **47**, 3991 (1967).
- (32) E. Wada, Y. Taru, and S. Tatsumiya, *Rep. Prog. Polym. Phys. Jpn.*, **15**, 41 (1972).
- (33) There are two recent light-scattering investigations on polystyrene in the range of high molecular weights: D. McIntyre, L. J. Fetters, and E. Slagowski, *Science*, **176**, 1041 (1972); A. Burmeister and G. Meyerhoff, *Ber. Bunsenges. Phys. Chem.*, **78**, 1366 (1974). Unfortunately, both papers did not contain any experimental data from which we can objectively evaluate the accuracy of the data. In addition, the distribution of molecular weight of the sample is not sharp in the former, and the sensitivity of the instrument seems insufficient in the latter.

## Equation of State of Poly(dimethylsiloxane) up to 800 kg/cm<sup>2</sup>

Kenji Kubota\* and Kazuyoshi Ogino

Department of Pure and Applied Sciences, College of General Education,  
University of Tokyo, Komaba, Meguro-ku, Tokyo, 153, Japan.

Received November 28, 1977

**ABSTRACT:** Isotherms of poly(dimethylsiloxane) (molecular weight  $5.10 \times 10^4$ ) were measured at various temperatures and up to 800 kg/cm<sup>2</sup>. The  $P$ - $V$ - $T$  relations were described by the Tait equation. The pressure dependence of the characteristic parameters of the equation of state of the Flory theory was examined from these  $P$ - $V$ - $T$  relations. Pressure dependences were comparatively large. At high pressure the equation of state of the Flory theory cannot adequately represent the  $P$ - $V$ - $T$  behavior of the polymer system.

The present investigation was undertaken with the objective of examining the properties of the equation of state and the applicability of the Flory theory<sup>1</sup> to polymers under pressure. During the last 10 years, the theory of polymer solutions developed by Flory,<sup>1,2</sup> Patterson,<sup>3</sup> and the others<sup>4,5</sup> has clarified the importance of "equation-of-state" effects. These effects can be attributed to the free volume difference between the solvent and the polymer. The equation-of-state characteristics of bulk amorphous polymer are of intrinsic interest apart from the analysis of the properties of the solutions. Especially, poly(dimethylsiloxane) has an extraordinarily large thermal expansion coefficient and isothermal compressibility compared with other polymers. Many investigations about temperature dependences of equation-of-state parameters of polymers are reported, but data on the pressure dependences of these under elevated pressure are scarce.

In this work, from the density of poly(dimethylsiloxane) at various temperatures, the pressure dependence of the characteristic parameters of the equation of state of the Flory theory were examined, and various premises of the Flory theory were examined at elevated pressure.

### Experimental Section

Poly(dimethylsiloxane) (PDMS) was from the Shin-Etsu Chemical Co., with 6000 CS. The viscosity average molecular weight determined by the equation of Barry<sup>6</sup> ( $\log \eta_{CS}^{25^\circ C} = 1.00 + 0.0123M^{0.5}$ ) was  $5.10 \times 10^4$ . PDMS was sufficiently evacuated before measurements in order to remove volatile constituents.

The  $P$ - $V$  isotherms were measured by a piston-cylinder type high-pressure cell. The cell is made of beryllium-copper alloy and its capacity is ca. 10 cm<sup>3</sup>. Pressure was applied by compressing the test

sample directly, and the volume change was determined from the piston displacement, the accuracy of which was  $\pm 2 \times 10^{-3}$  cm<sup>3</sup> (0.02%). The pressure cell was immersed in a silicon oil bath, and the temperature was regulated to within 0.01 °C. Pressure was measured using a manganin gauge and a home-made Kelvin double bridge. The temperature of the test sample in the pressure cell was checked by a platinum wire resistor.

The isothermal compressibility of benzene was measured for calibration and was compared with the data of Gibson et al.<sup>7</sup> The largest discrepancy was 1% in the range of 20–60 °C.

This apparatus yields only the volume change relative to that at atmospheric pressure. Therefore, it is necessary to know the specific volume of PDMS at atmospheric pressure, and the data of Shih and Flory<sup>8</sup> were used for this purpose.

### Results and Discussion

Relative volumes were measured as a function of pressure and temperature over the range of 1–800 kg/cm<sup>2</sup> and 29–60 °C. Five isotherms (29.0, 32.5, 38.4, 49.0, and 60.0 °C) were obtained. The changes in volume relative to those at atmospheric pressure at various temperatures are given in Table I, and some of them are shown in Figure 1.

At all temperatures, the observed  $P$ - $V$  behavior can be represented by the equation proposed by Tait,

$$V/V_0 = 1 - C \ln(1 + P/B) \quad (1)$$

where  $V$  is the specific volume at pressure  $P$  and temperature  $T$ ,  $V_0$  is the specific volume at atmospheric pressure and the same temperature  $T$ ,  $C$  is a dimensionless constant, and  $B$  is a volume-independent function of temperature. The theoretical basis of this equation has been discussed<sup>9</sup> and it is